INTRACELLULAR MICROELECTRODE MEASUREMENTS IN SMALL CELLS EVALUATED WITH THE PATCH CLAMP TECHNIQUE

CAN INCE,*‡ ED VAN BAVEL,‡ BERT VAN DUIJN,‡ KEES DONKERSLOOT,‡ ANNEMIEK COREMANS,‡ DIRK L. YPEY,‡ AND ALETTUS A. VERVEEN‡

Department of Infectious Diseases, University Hospital, Rijnsburgerweg 10, 2333 AA Leiden, The Netherlands; and ‡Department of Physiology, University of Leiden, Wassenaarseweg 62, 2333 AL Leiden, The Netherlands

ABSTRACT Microelectrode penetration of small cells leads to a sustained depolarization of the resting membrane potential due to a transmembrane shunt resistance (R_s) introduced by the microelectrode. This has led to underestimation of the resting membrane potential of various cell types. However, measurement of the fast potential transient occurring within the first few milliseconds after microelectrode penetration can provide information about pre-impalement membrane electrophysiological properties. We have analyzed an equivalent circuit of a microelectrode measurement to establish the conditions under which the peak of the impalement transients (E_p) approaches the pre-impalement resting membrane potential (E_m) of small cells most closely. The simulation studies showed that this is the case when the capacitance of the microelectrode is low and the membrane capacitance of the cell high. In experiments performed to assess the reliability of E_p as a measure of E_m, whole-cell patch clamp measurements were performed in the current clamp mode to monitor, free from the effects of R_s, E_m in cultured human monocytes. Microelectrode impalement of such patch clamped cells and measurement of E_p made it possible to detect correlation between E_p and E_m and showed that for small cells such as human monocytes E_p is on average 6 mV less negative than the resting membrane potential.

INTRODUCTION

Since the introduction of the patch clamp technique into electrophysiology, detailed studies can be done on the electrical properties of small cell types (1, 2). An important electrical property that needs to be determined in such cells is the resting membrane potential (rmp). For large cells (diameters $>>50\ \mu m$) this can be done by use of intracellular microelectrode recordings. Although care must be taken to avoid leakage of the microelectrode filling into the cell (3), the steady state potential measured can be taken to be the value of the rmp. Application of this method to small cells can, however, lead to underestimation of the rmp due to the introduction of an electrical transmembrane shunt resistance R_s created by the hydration mantle surrounding the microelectrode. The resistance of such a water layer between glass and cell membranes has been estimated to lie between 50 and 200 MΩ (1). A patch clamp measurement does not have this drawback, because of the achievement of a tight seal (giga-seal) between the patch electrode and the cell membrane (1), which means that (in the whole-cell current clamp mode) membrane potential measurements on small cells are not affected by electrode-induced transmembrane shunts (1, 4). However, use of this method to determine the value of the rmp of a cell has the disadvantage that during whole-cell recording the inside of the cell is perfused by the contents of the patch pipette. Since the exact composition of the intracellular fluid is often unknown, use of an arbitrary pipette fluid can alter the rmp with respect to its value before the measurement. Thus, despite the acquisition of the patch clamp technique, a method for direct measurement of the rmp of small cells is still needed.

Lassen et al. (5) introduced a method for estimation of the pre-impalement rmp of small cells which takes the presence of the microelectrode-induced shunt into account. This method measures the fast potential transient seen in the first few milliseconds after microelectrode penetration. This impalement transient consists of a fast negative-going potential transient reaching a peak value, E_p, followed by a depolarizing transient to a steady state potential E_s. The observation that in a number of cell types E_p is more negative than E_s indicated that the rmp of these cells is more negative than had been assumed on the basis of E_s measurements (3, 5, 6–8). Although impalement transient measurements show whether a steady state measurement is affected by the presence of an R_s (i.e., if E_p is more negative than E_s), uncertainty exists concerning the accuracy of impalement transient measurements for determining the value of the pre-impalement rmp. Use of the patch clamp technique in combination with microelectrode

impalements now provides an experimental method to help resolve this uncertainty.

The present study was performed to investigate the extent to which E_p is a good measure of the resting membrane potential of small cells. An equivalent electrical circuit and mathematical analysis were used to investigate the nature of the impalement transient. Patch clamp measurements in the whole-cell current clamp mode combined with microelectrode impalements were applied to cultured human monocytes and used to establish the relation between the pre-impalement rmp and the peak of the impalement transient measured upon microelectrode entry. The results show that under certain conditions E_p is a good measure of the resting membrane potential prior to cell impalement. Preliminary results of this study have been reported elsewhere (4).

MATERIALS AND METHODS

Peripheral blood monocytes from healthy human donors were cultured on flying coverslips in petri dishes for 1–3 wk (7). Monocytes cultured in this way differentiate into macrophage-like cells reaching cell diameters between 10 and 40 μm. The glass coverslips with adherent cells were mounted to a Teflon dish and placed on the stage of an inverted microscope where microelectrode and patch clamp measurements were made at an objective magnification of 100 × with oil immersion optics (9). The cells were bathed in a solution composed of 150 mM NaCl, 3 mM KCl, 1 mM $MgCl_2$, 4 mM $CaCl_2$, and 10 mM HEPES-NaOH (pH 7.2). Measurements were made at room temperature.

Membrane potential measurements were performed with microelectrodes and patch electrodes and a dual-input Series 700 Micro Probe 750 microelectrode pre-amplifier (World Precision Instruments, New Haven, CT). Fine-tipped microelectrodes (tip diameters <0.2 μm), filled with 4 M K-acetate had resistances between 50 and 300 MΩ. Capacitance compensation was used to obtain microelectrodes with rise times <0.1 ms. Cells were impaled by means of a piezo-stepper device (Piezo-stepper P-2000, Physik Instruments (PI), Waldbronn-Karlsruhe, Federal Republic of Germany). Patch electrodes were drawn from thin-walled borosilicate glass and giga-seals were made according to Hamill et al. (1). Patch pipettes were filled with a solution composed of 143 mM KCl, 2 mM $MgCl_2$, 2 mM $CaCl_2$, 10 mM HEPES-KOH (pH 7.2), and sometimes buffered with 10 mM EGTA to bring Ca^{2+} to intracellular levels. This solution was also used as filling for the reference pool and microelectrode holder. The reference pool was connected to the bathing solution with a salt bridge filled with extracellular solution. Membrane potentials were measured with respect to the base line of either the microelectrode or patch electrode before cell contact being made.

RESULTS

Mathematical Analysis of a Microelectrode Measurement

An intracellular potential measurement by use of a microelectrode can be represented by the equivalent circuit shown in Fig. 1 *A*, in which an instantaneous electrical shunt, R_s, is introduced by the electrode upon cell entry. In the equivalent circuit, cell impalement is simulated by closing switch *S*. The potential E_d is included to cover a possible diffusion potential created by the ionic concentration differences across the shunt (5). As can readily be seen from the equivalent circuit in Fig. 1 *A*, if R_s is of the order

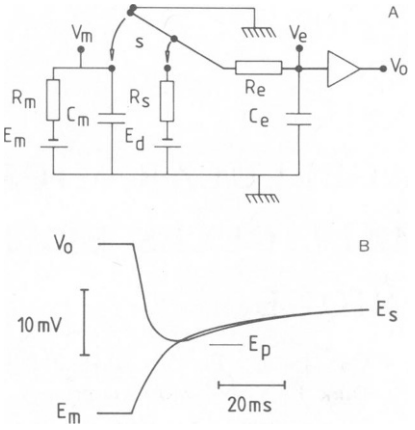

FIGURE 1 Equivalent electrical circuit representation of a microelectrode measurement where a transmembrane shunt is introduced by the microelectrode. (*A*) Cell parameters are: resting membrane potential, E_m; a membrane capacitance, C_m; and resistance, R_m. Electrode parameters are: an electrode resistance, R_e; and capacitance, C_e. The shunt introduced by the microelectrode has a resistance, R_s, and creates a diffusion potential, E_d. Cell impalement by the electrode is simulated by the closure of switch *S*. The potential measured at the microelectrode amplifier output is V_o; the intracellular potential is V_m, and the potential in the microelectrode is V_e. V_e is 0 before impalement (before switch *S* is closed) and V_m is equal to E_m. (*B*) A trace of the time course of V_o (*top*) and V_m (*bottom*) upon closure of switch *S* in the equivalent circuit. The circuit reproduces peak potential recordings which at V_o are seen as sharp negative-going deflections reaching a peak value E_p followed by a depolarizing transient to a steady state potential E_s. The time course of V_m crosses the peak transient at its level E_p. Scaled values of circuit parameters used here have the following values: R_m, 100 KΩ; C_m, 3 μF; R_e, 2.7 KΩ; C_e, 0.47 μF; R_s, 10 KΩ; and E_d, 0.

of or smaller than the cell membrane resistance R_m, the measured sustained potential E_s at the amplifier output V_o, will be less negative than the pre-impalement resting membrane potential E_m.

After reduction of the electrode time constant $T_e = (R_eC_e)$ by capacitance compensation, an impalement transient can be measured, which can provide information about the pre-impalement electrical properties of small cells (5, 10). As can be seen in Fig. 1 *A*, the membrane capacitance C_m is charged to the value E_m before cell impalement (i.e., when switch *S* is open). When the microelectrode is driven into the cell and R_s is introduced, C_m will discharge from E_m to a new steady-state potential level E_s. If the response time of the microelectrode is sufficiently rapid, this discharge of C_m can be monitored at V_o. Under these conditions the potential transient seen during the first few milliseconds immediately after microelectrode penetration, is characterized by a rapid negative-going potential transient (determined by T_e) that reaches a peak value E_p, followed by a slower depolarizing transient due to the discharge of C_m (Fig. 1 *B*). The closest estimate of E_m based on direct measurement by microelectrode impalement is therefore E_p. Although E_p provides a better estimate of E_m than E_s does, it remains an underestimation of E_m (due to limitations imposed by T_e). Therefore, a

method by which the value of E_m can be best determined is still needed.

A simplified model of the impalement transient proposed by Lassen et al. (5) predicts that E_m can be calculated by exponential extrapolation of the depolarizing tail of an impalement transient back to the moment of cell penetration under the assumption that R_s stays constant during impalement. Such an extrapolation is possible due to the absence in the model of the capacitative load imposed by C_e on the discharge of the membrane. As a consequence, in Lassen's model the time course of the discharge of the membrane potential upon closure of switch S does not intersect the peak of the impalement transient measured at V_e (Fig. 1 *A*). As can be seen in Fig. 1 *B* where both the discharge of the membrane potential and the impalement transient recorded at V_e are shown, this is not the case. This illustrates that the impalement transient is not fully described by the model of Lassen et al. The following analysis shows that under certain conditions the value of E_p itself is a good estimate of E_m.

A mathematical expression for the impalement transient is obtained when Kirchhoff's laws are applied to the circuit in Fig. 1 *A*. According to these laws the sum of the currents flowing through R_m, C_m, R_s, and R_e after closure of the switch at time $t = 0$, must be zero. Under the assumption that amplifier A has ideal input characteristics (i.e., $V_o = V_e$), the current through R_e equals the current through C_e. Substitution of potentials and components for the currents which flow after closure of switch S gives an expression relating the potential at the input of the amplifier V_e to the membrane potential before impalement (E_m)

$$T_m T_e \frac{d^2V_e}{dt^2} + (T_m + T_c + \beta T_e)\frac{dV_e}{dt} + \beta V_e = \frac{R_m}{R_s} E_d + E_m \quad (1)$$

in which $T_m = R_m C_m$, $T_e = R_e C_e$, $T_c = R_m C_e$, $\beta = (R_s + R_m)/R_s$, and where E_d is the diffusion potential and R_s the resistance of the microelectrode-induced shunt. In the steady state situation (i.e., when $t \rightarrow \infty$), Eq. 1 reduces to

$$V_e = E_s = \frac{E_m R_s + E_d R_m}{R_m + R_s} \quad (2)$$

where E_s is the steady state potential measured by the microelectrode. The accuracy of E_s as a measure of E_m depends on whether R_s is sufficiently large relative to R_m, and on the magnitude of E_d. For measurements where $R_s >> R_m$, Eq. 2 reduces to $E_s = E_m$. Under such conditions steady state measurements are free from the ill effect of R_s. Such a situation only occurs in patch clamp measurements where the giga-seal ensures that $R_s >> R_m$, or in intracellular microelectrode measurements from very large or electrically coupled cells, where $R_m << R_s$. When R_s is in the order of magnitude of R_m, however, as is the case in most studies on small isolated cells, E_s underestimates E_m and contains a considerable contribution from E_d (see Eq. 2).

Measurement of the peak potential E_p provides a more accurate measure of E_m than does E_s (5, 7). To determine how good an estimate E_p is of E_m, values of E_p were calculated for different E_m. To gain insight into the drawbacks of the use of E_p to measure E_m, unfavorable values of parameters were chosen on purpose. E_p was then calculated by solving Eq. 1. Since all coefficients in Eq. 1 are positive, the solution of Eq. 1 will be of the form:

$$V_e = A \exp(Q_1 t) + B \exp(Q_2 t) + E_s. \quad (3)$$

The factors Q_1, Q_2, A, and B can be calculated from the characteristic equation and the initial conditions ($V_e = 0$ and $dV_e/dt = E_m/T_e$ at time $t = 0$). This gives for factors A, B, Q_1, and Q_2

$$A = \frac{E_m/T_e + Q_2 E_s}{Q_1 - Q_2} \quad \text{and} \quad B = -\frac{E_m/T_e + Q_1 E_s}{Q_1 - Q_2} \quad (4)$$

Q_1, Q_2

$$= \frac{(T_m + \beta T_e + T_c) \pm [(T_m + \beta T_e + T_c)^2 - 4\beta T_m T_e]^{1/2}}{(-2T_m T_e)} \quad (5)$$

A peak potential, E_p, will then be measured at V_o when dV_e/dt is equal to zero. This occurs when the following inequality is satisfied

$$\frac{E_d}{E_m} < -\frac{1 + (R_s/R_m)(1 + Q_1 T_e)}{Q_1 T_e} \quad (6)$$

For parameter values that do not satisfy this inequality, the solution of Eq. 1 will be strictly monotonic and therefore approach E_s but not overshoot it. This latter situation occurs, for example, if $T_e >> T_m$. For the general case, however, when $T_e < T_m$ in small cells, the condition of Eq. 6 is satisfied and a peak potential will be measured. The time t_p it takes V_e to reach E_p is then given by

$$t_p = \frac{\log_e - (Q_1 A/Q_2 B)}{Q_2 - Q_1}. \quad (7)$$

By substitution of Q_1, Q_2, A, and B and t_p in Eq. 3, the value of E_p is given by

$$E_p = A(-Q_1 A/Q_2 B)^{Q_1/(Q_2 - Q_1)} + B(-Q_1 A/Q_2 B)^{Q_2/(Q_2 - Q_1)} + E_s \quad (8)$$

To investigate the relation between E_p and E_m, parameter values were varied and E_p was calculated for different values of E_m. Since capacitance compensation can give electrode rise times <0.1 ms, 100 MΩ electrode here has a residual capacitance of 1 pF.

To assess the parameter sensitivity of E_p, the first circuit parameters varied were the membrane resistance R_m and the diffusion potential E_d. Variation of R_m between 200 MΩ and 5 GΩ and of E_d between 0 and −30 mV showed that these parameters had little effect on the value of E_p

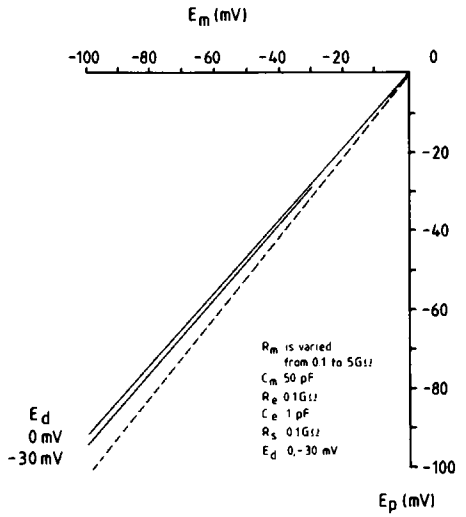

FIGURE 2 Effect of R_m and E_d on the relationship between the peak potential E_p and the pre-impalement membrane potential E_m. Two E_d values were compared (0 and -30 mV). R_m was varied between 200 MΩ and 5 GΩ for $E_d = 0$ as well as for $E_d = -30$ mV, but had little influence on E_p/E_m. The cell and electrode parameters are indicated. E_p is not defined for values of E_m less negative than -31 mV for the case where E_d is -30 mV (see Eq. 6 in text).

(Fig. 2). Since R_m and E_d do not significantly affect E_p, the factors to be investigated further were C_m, the membrane capacitance, and R_s, the shunt resistance, as well as R_e and C_e.

As can be seen from Fig. 3, the value of E_p is strongly dependent on the membrane capacitance, C_m. This could be expected because for a fixed value T_e, E_p will approach E_m more closely when C_m discharge slowly (i.e., with large C_m) than it would if C_m discharged rapidly (small C_m). Thus E_p measurements become less accurate for very small

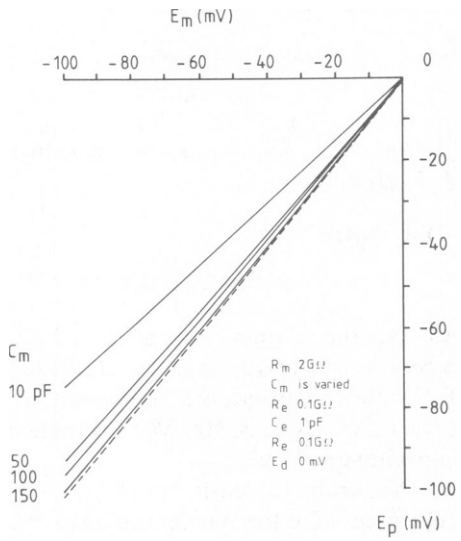

FIGURE 3 The peak of the impalement transient, E_p, is dependent on the value of the membrane capacitance C_m.

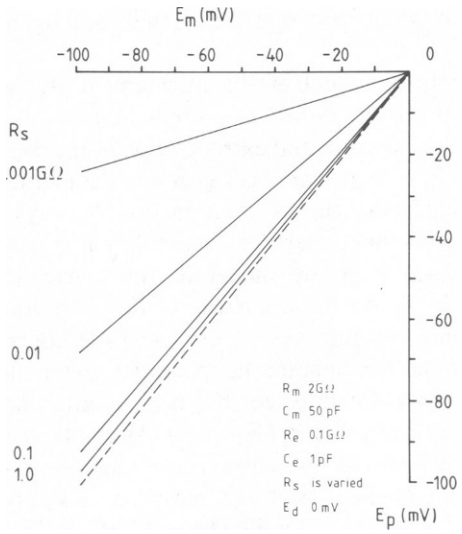

FIGURE 4 The influence of the microelectrode-induced shunt resistance R_s on the peak of the impalement transient E_p.

cells, unless very low C_e electrodes can be used. Fig. 4, where E_d is taken as 0 mV, shows that E_p approaches E_m less closely for smaller values of R_s. Furthermore, with lower values of R_s the dependency of E_p on E_d increases (Table I). The value of E_p/E_m depends strongly on T_e ($= R_eC_e$). For example, in Table I for $E_d = 0$ and $R_s = 1$ GΩ, E_p/E_m is equal to 0.97 for $T_e = 0.1$ ms, whereas for a cell with the same parameters but with a T_e of 0.5 ms, E_p/E_m is only equal to 0.77. This observation underscores the need to use maximum capacitance compensation of the microelectrode. Not only the value of the product of $R_e C_e$, but also the individual values of R_e and C_e will influence E_p/E_m. This is illustrated in Table II, where the effect of C_e on E_p/E_m is shown for a constant product $R_e C_e$ (T_e).

Experimental Evidence

In the previous section it was shown that according to theoretical criteria the value of E_p can provide a good measure of E_m. To verify this prediction experimentally, patch clamp measurements (which do not suffer from the effects of R_s) were made in the whole-cell current clamp configuration under giga-seal (i.e., $R_s > 10$ GΩ) conditions (1) combined with microelectrode impalement of the same

TABLE I
THE EFFECT OF R_s AND E_d ON E_p/E_m

E_d	$R_s = 1$ MΩ	$R_s = 10$ MΩ	$R_s = 100$ MΩ	$R_s = 1$ GΩ
mV	E_p/E_m	E_p/E_m	E_p/E_m	E_p/E_m
0	0.25	0.66	0.91	0.97
−10	0.27	0.68	0.91	0.97
−20	0.31	0.70	0.92	0.97
−30	0.35	0.72	0.92	0.97

R_m, 2 GΩ; C_m, 50 pF; R_e, 100 MΩ; C_e, 1 pF; E_p/E_m only holds for values of E_m which satisfy Eq. 6.

TABLE II
THE EFFECT OF R_e AND C_e ON E_p/E_m

R_e	C_e	E_p/E_m
50 MΩ	10 pF	0.68
100 MΩ	5 pF	0.72
500 MΩ	1 pF	0.76
1 GΩ	0.5 pF	0.77
5 GΩ	0.1 pF	0.77

R_m, 2 GΩ; C_m, 50 pF; $T_e = R_eC_e = 0.5$ ms; E_d, 0; R_s, 100 MΩ.

cell. Subsequently the value of E_m can be correlated with E_p as measured by the penetrating microelectrode.

Cultured human monocytes were used for the experiments in which patch clamp measurements were combined with microelectrode impalement. After a giga-seal had been established in current clamp mode, the patch was broken by application of an extra suction pulse to the patch electrode, thereby obtaining a whole-cell measurement where E_m was recorded. Current pulses applied via the patch electrode gave a double exponential response reflecting the rise time of the patch electrode in series with the membrane. From such current pulse responses the values of R_m and C_m could be determined and revealed a wide spread of values of R_m (20 MΩ–5 GΩ) and C_m (10 pF–90 pF), reflecting the heterogeneity of cell sizes in these human monocyte cultures.

As soon as a stable membrane potential, E_m, was recorded from the patch electrode (indicating equilibrium between original cell content and perfusate), the microelectrode was driven into the cell and potentials from both electrodes were recorded. In records made on a slow time-scale (where the impalement transient cannot be seen due to the slow response of the chart recorder), the depolarizing effect of the microelectrode-induced shunt can be seen as a sustained depolarization with respect to E_m prior to impalement (Fig. 5 *A*). For the example shown in Fig. 5 *A*, the membrane resistance measured before microelectrode impalement, 136 MΩ, and the value of the impaled membrane resistance measured immediately after impalement (i.e., after the introduction of R_s), 58 MΩ, gives a value of 101 MΩ for R_s. Substitution of this value of R_s into Eq. 2 together with the values of E_m (−91 mV) and E_s (−51 mV) from Figs. 5 *A* and *B*, gives a value for the shunt induced diffusion potential E_d of −5 mV. This value is close to that predicted by Lassen et al. (−9 mV) for ascites tumor cells (5). The record in Fig. 5 *A* illustrates that cautious use of steady-state membrane potential measurements on high resistance cells measured with microelectrodes is advisable. Another estimate of R_s was obtained by impalement of a cell under whole-cell voltage clamp conditions. The cell was held at −50 mV and the excess current drawn from the voltage clamp upon impalement was measured. Under the assumption that this excess current resulted solely from the introduction of R_s, values of 260 and 157 MΩ were calculated for R_s in two cases.

In Fig. 5 *B* the microelectrode impalement transient is recorded on a fast time scale simultaneously with the depolarization of the membrane recorded by the patch electrode. The peak of the impalement transient equals the value of E_m before microelectrode entry. Such large values of E_p were never measured in impalements in intact cultured human monocytes (range, −30 and −50 mV) indicating that perfusion of the cell by the patch filling affected the rmp of this cell. In Fig. 5 *C*, experiments of the type shown in Figs. 5 *A* and *B* are shown graphically, the values of E_m measured by the patch electrode prior to microelectrode impalement being plotted against each subsequent E_p value measured by the microelectrode in 16 cells. These results show that E_p follows the value of E_m to within 10 mV.

Membrane potential values may be influenced by a small change in the diffusion potential at the fluid interface of the electrode tip as the electrode establishes contact with the intracellular solution. For our microelectrode measurements we found no significant change in baseline when exchanging the extracellular for the intracellular fluid used (taking the change in diffusion potential at the salt bridge into account). For patch electrode measurements, however, the liquid junction potential that exists at the patch electrode tip (the patch electrode filling being ~3 mV electronegative with respect to the bathing solution) is abolished when a whole-cell measurement is made. This means that the absolute membrane potentials could be ~3 mV more negative than those measured with respect to the baseline of the patch electrode before cell contact. Correction of the membrane potentials measured by the patch electrode for this 3 mV change in diffusion potential leads to E_p being on average 6 mV (SD = 2, n = 16) less negative than the absolute membrane potential.

DISCUSSION

The present results show that the peak value, E_p, of the rapid potential transient seen upon microelectrode impalement, can be used as a good measure of the resting membrane potential (E_m) of small cells. The evidence is supported by equivalent circuit analysis as well as by patch clamp measurements in combination with microelectrode impalements on cultured human monocytes.

The theoretical analysis showed that the closeness of E_p to E_m is determined mainly by the values of the membrane capacitance C_m, the electrode capacitance C_e, and the shunt resistance R_s caused by the microelectrode. Larger values of C_m and R_s and smaller values of C_e enhance the reliability of using E_p as a measure of E_m. These parameters can be experimentally manipulated to obtain favorable conditions for E_p values to more closely approach values of E_m.

The membrane capacitance, C_m, can be increased if large cells are available. These can be obtained by, for example, x-irradiation of a dividing cell line (10). Since irradiation halts cell division but not necessarily cell

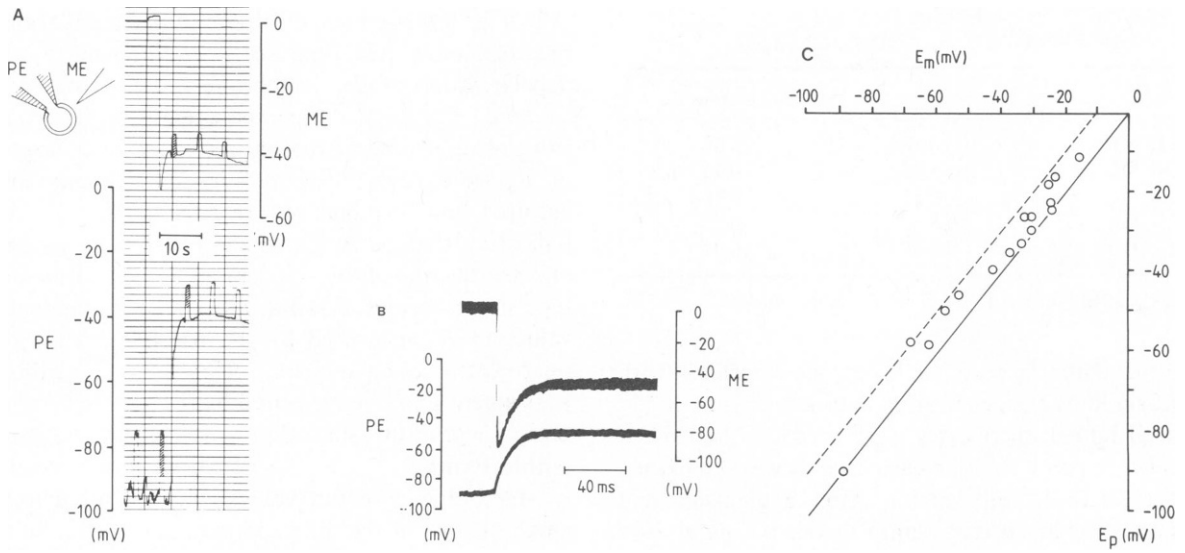

FIGURE 5 Simultaneous membrane potential recordings on a cultured human monocyte from a patch electrode in the whole-cell current clamp mode and an intracellular microelectrode, showing the effect of the introduction of a microelectrode-induced transmembrane shunt, R_s. (*A*) The potential transients, seen on a slow time scale as the microelectrode impales the cell, show the steady state effect of the introduction of R_s by the microelectrode. The *bottom* trace represents the potential measured by the patch electrode (*PE*) and the *top* trace is the potential measured by the microelectrode (*ME*) upon impalement of the cell by the microelectrode. The introduction of the microelectrode leads to a depolarization of the membrane potential from −91 mV to about −50 mV. Membrane resistance is measured by passing 0.1 nA pulses through the *PE* before the *ME* impalement. The pulse response measured by the *PE* reflects the membrane resistance (shaded, 136 MΩ) and the series resistance of the *PE* (48 MΩ). Measurement of the membrane resistance (58 MΩ) after *ME* impalement, shows that the *ME* has introduced an R_s of 101 MΩ. The response to the injected current pulse via the *PE* as measured by the *PE* after *ME* penetration reflects the series resistances of the *PE* and the membrane. The *ME* only measures the resultant membrane resistance. The patch electrode was filled with K^+-saline without added EGTA. The two potential transients are slightly shifted in time due to the distance between the pens of the two channels of the recorder. (*B*) The potential transients measured on a fast time scale by the *PE* (*bottom* trace) and by the *ME* (*top* trace) at the moment of cell impalement of the records shown in *A*. The peak potential measured by the *ME* (−91 mV) equals the pre-impalement membrane potential (−91 mV) measured by the *PE*. The vertical positions of the two transients have been shifted to make both transients visible. (*C*) The relationship between the pre-impalement membrane potential E_m measured by the *PE* and the peak potential E_p by the *ME* in 16 experiments. The plot shows that E_p provides an estimate of the pre-impalement membrane potential within 10 mV (dashed line). R_m ranged in these measurement from 20 MΩ to 5 GΩ and C_m from 10 to 90 pF.

growth, culture of irradiated cells yields giant cells (11). This process did not alter the value of the resting membrane potential of a murine macrophage or of a fibroblast cell line (10). Another way to obtain large cells is by prolonged culture of cells: the original size of mononuclear phagocytes, e.g., mouse peritoneal macrophages and human monocytes, increases by a factor of 2 to 5. Other methods such as cell fusion (12) can also be considered for this purpose. However, it should be kept in mind that use of techniques to obtain large cells may change the functional properties of cells.

The electrode capacitance, C_e, can be decreased by optimal use of capacitance compensation. Fabrication of electrodes with a wider-angle taper gives electrodes having a closer resemblance to a single RC network, which means that capacitance compensation can be used optimally. Smaller-tip angle electrodes have a more distributed RC network, which limits the use of capacitance compensation. Wider angle electrodes have, however, the disadvantage that such electrodes probably decrease the value of R_s and thus abolish the advantage gained by lowering the C_e. An alternative method for lowering C_e could be achieved by sylgard coating of the microelectrode. Thus, the general notion that high-resistance microelectrodes leads to more reliable membrane potential measurements is not true for peak potential measurements, because it is the value of the electrode capacitance which mainly determines the usefulness of E_p as a measure of E_m.

Measurement of the impalement transient can facilitate electrophysiological investigations into single cells in various ways. Measurement of E_p can be important, for example, for establishing whether sustained potential measurements done with intracellular microelectrodes suffer from the effects of a microelectrode-induced shunt resistance R_s. Peak potential measurements have thus enabled a number of authors to establish that the resting membrane potential of different cell types is more negative than had previously been thought on the basis of intracellular steady-state potential measurements (5–8, 13). Furthermore, analysis of the shape of the impalement transient in macrophages and fibroblast cell lines revealed that the membrane potentials of these cells do not oscillate prior to microelectrode entry as they can do following microelectrode entry (10).

Measurement of E_p after ion channel measurements in the cell-attached patch configuration provides a basis for correction of the I–V curves of ion channels for the contribution of E_m, thereby enhancing the usefulness of cell-attached patch measurements. We used this method to establish the presence of K^+ channels in cultured human monocytes (4). Measurements of the E_p values of a population of cells in culture allows investigation of the effect of various conditions on the average resting membrane potential of the population. In this way peak potential measurements were used to identify the presence of a Na/K pump in cultured human monocytes (14). It is concluded that measurement of the peak potential offers a useful and reliable method to establish the resting membrane potential of small cells.

The authors are grateful to Prof. R. van Furth, and Dr. P. C. J. Leijh for continued support and for critical reading of the manuscript. We thank Joke van de Gevel for culture of cells.

The experiments described in the present study were performed at the Department of Physiology, University of Leiden.

C. Ince is supported by the Foundation for Medical Research (FUNGO), which is subsidized in part by the Netherlands Organization for the Advancement of Pure Research (ZWO).

Received for publication 28 August 1985 and in final form 25 June 1986.

REFERENCES

1. Hamill, O. P., A. Marty, E. Neher, B. Sakmann, and F. J. Sigworth. 1981. Improved patch-clamp techniques for high resolution current recording from cells and cell-free membrane patches. *Pfluegers Arch. Eur. J. Physiol.* 391:85–100.
2. Neher, E., and B. Sackman. 1976. Single channel currents recorded from membrane of denervated frog muscle fibres. *Nature (Lond.).* 260:799–802.
3. Blatt, M. R., and C. L. Slayman. 1983. KCl leakage from microelectrodes and its impact on the membrane parameters of a nonexcitable cell. *J. Membr. Biol.* 72:223–234.
4. Ince, C., and D. L. Ypey. 1985. Membrane hyperpolarizations and ionic channels in cultured human monocytes. *In* Mononuclear Phagocytes. Characteristics, Physiology and Function. R. van Furth, editor. Martinus Nijhoff Publishers, Boston, Dordrecht, Lancaster. Chapter 39. 369–377.
5. Lassen, U. V., A. M. T. Nielsen, L. Pape, and L. O. Simonsen. 1971. The membrane potential of Ehrlich ascites tumor cells. Microelectrode measurements and their critical evaluation. *J. Membr. Biol.* 6:269–288.
6. Chambers, E. L., and J. de Armendi. 1979. Membrane potential, action potential and activation potential of eggs of the sea urchin, *Lytechinus variegatus. Exp. Cell Res.* 122:203–218.
7. Ince, C., D. L. Ypey, R. van Furth, and A. A. Verveen. 1983. Estimation of the membrane potential of cultured macrophages from the fast potential transient upon microelectrode entry. *J. Cell Biol.* 96:796–801.
8. Lassen, U. V. 1972. Membrane potential and membrane resistance of red cells. *In* Oxygen Affinity of Hemoglobulin and Red Cells Acid Base Status. M. Rorth and and P. Astrup, editors. Munksgaard, Copenhagen.
9. Ince, C., J. T. van Dissel, and M. M. C. Diesselhoff-den Dulk. 1985. A Teflon culture dish for high magnification observations and measurements in single cells. *Pfluegers Arch. Eur. J. Physiol.* 403:240–244.
10. Ince, C., P. C. J. Leijh, J. Meijer, E. van Bavel, and D. L. Ypey. 1984. Oscillatory hyperpolarizations and resting membrane potentials of mouse fibroblast and macrophage cell lines. *J. Physiol. (Lond.).* 352:625–635.
11. Whitemore, G. F., J. E. Till, R. B. L. Gwatkin, L. Siminovitch, and A. F. Graham. 1958. Increase of cellular constituents in x-irradiated mammalian cells. *Biochim. Biophys. Acta.* 30:583–590.
12. Persechini, P. M., E. G. Araujo, and G. M. Oliveira-Castro. 1981. Electrophysiology of phagocytic membranes: induction of slow hyperpolarizations in macrophages and macrophage polykaryons by intracellular calcium injection. *J. Membr. Biol.* 61:81–90.
13. Bretschneider, F. 1985. Transient measurement of the membrane potential of receptor cells of an ampullary electroreceptor in the transparent catfish. *J. Physiol. (Lond.).* 366:17P.
14. Ince, C., P. C. J. Leijh, B. Thio, B. van Duijn, and D. L. Ypey. 1985. Identification of a Na/K pump in cultured human monocytes. *J. Physiol. (Lond.).* 366:90P.